

## Photobioreactor Design and Fluid Dynamics

J. C. Merchuk,\* F. Garcia-Camacho, and E. Molina-Grima

Department of Chemical Engineering, University of Almería, Spain

\*On sabbatical leave from Department of Chemical Engineering, Ben-Gurion University, Israel

Original scientific paper

Received: July 29, 2007

Accepted: October 24, 2007

Photobioreactor design is a subject of great relevance for the attainment of a sustained development in modern technology, and has also considerable interest from the basic scientific and technologic point of view. The aim of the present review paper is presenting and comparing some of the recent attempts by the authors of modelling photosynthesis in reactors. A short inspection of the kinetic models proposed for photobioreactor design is done, and some examples of the integration of such kinetic models and bioreactor fluid dynamics in the modelling of photobioreactors are presented.

*Key words:*

Photosynthesis, photoinhibition, mathematical modelling, photobioreactors

### Introduction

Photosynthesis has been studied for a very long time, being this justified by the vital importance it has for the very existence of life on earth. The exploitation by man of the many opportunities that photosynthesis offers for the production of valuable biochemicals is based on the accumulated knowledge on the matter, and it is one of the most interesting and challenging problems in biochemical engineering. Moreover, the production of bio-fuels from algal biomass is one of the most ambitious aims in the quest for a sustainable ecological balance worldwide and has gained lately much attention. In Fig. 1, a sketch is shown to indicate the place of algal culture for bio fuels in the overall fuel-energy scheme. The overall aim is the diminution of environmental contamination, which would be attained by recycling part of the CO<sub>2</sub> produced in the utilization of fossil fuels for energy generation.

In spite of the huge interest in bio fuel production from algae, the economic aspects of the pro-

cess are still to be satisfactorily solved. Therefore, the most important engineering aim in this area is the development of a process that provides biomass rich in chemical energy at the lowest cost. Assuming the best algal species for the process is identified and selected, the next quest remaining is an optimal design of the bioreactor. Such optimization requires a deep knowledge of the system, and a mathematical model that represents it satisfactorily. The model should therefore be able to represent the basic characteristics of algal kinetics, being still simple enough to allow a relatively easy computational approach.

### The kinetic model

A satisfactory kinetic model is the base for any bioreactor calculation, design or optimization. In the case of photosynthetic cells, much is known about the basics of the photochemical and biochemical mechanisms involved, and much of it can be found in standard textbooks and periodicals. However, the picture emerging after inspection of this basic knowledge renders the description of a system that is much too complicated for direct utilization in engineering calculations. On the other hand, the actual behaviour of the photosynthetic cultures is very complicated, it includes many variables, and the different steps in the processes have time-constants that differ in orders of magnitude. Therefore, it is difficult to represent the behaviour of a culture by simple kinetic expressions. This is specially so when the dynamic behaviour of the cultures has to be considered, as is the case of the integration of fluid-dynamics with photosynthesis that will be ex-

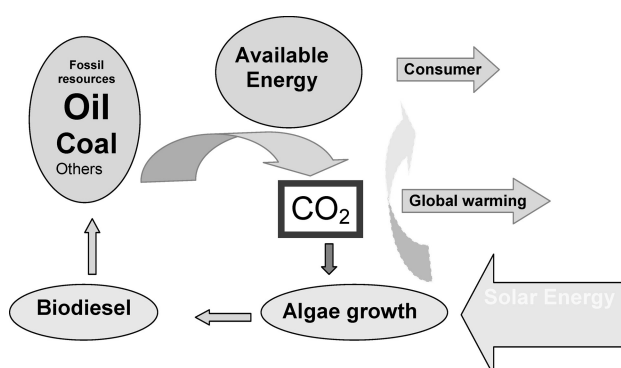


Fig. 1 – Carbon recycle as an ecological measure

plained further on. Because of this, all of the mathematical models of photosynthesis available in the literature are based in the lumping of a large amount of biochemical reactions into simpler steps or into hypothetical concepts, which aim at representing the behaviour of the actual biochemical apparatus. The selection of a model is thus the result of the compromise between the “loyalties to biology”, that is, to the elements of the biochemical steps that are quite known in the photosynthetic process, and the computational burden resulting of a complex mathematical formulation.

The minimal requirement from a mathematical model is the prediction of the P-I curve. That is the dependence of the Photosynthesis rate on irradiance, with the easily measurable parameters usually called  $\alpha$ , the initial photosynthesis rate, and  $P_m$ , the maximal photosynthesis rate, at certain irradiance  $I_m$ . One of the earliest approaches is the Aiba equation, adopting the form of a substrate-inhibited enzymatic reaction to account for photoinhibition (Aiba, 1982).

$$\mu = \frac{\mu_{\max} I}{K_1 + I + K_i I^2} \quad (1)$$

This single equation gives a satisfactory result for photo-adapted systems operation at steady state. The only variable, illumination  $I$ , is extra-cellular, and the parameters can easily be found empirically, fitting to experimental data.

On the other hand, several much more sophisticated models aiming at the representation of the dynamic behaviour of photosynthetic cells and their capacity of adaptation to different illumination intensities have been proposed lately. Those models include as variables not only the irradiance, but also some intra-cellular variables as chlorophyll concentration, extent of light-damaged protein D1 in Photosystem II, nitrogen and carbon content in the cell (Geider et al, 1998; Harmon and Challenor, 1997; Pahlow, 2005; Smith et al, 2007; Marshall et al, 2000).

There is still another group of models of photosynthesis that can be situated between the previous two extremes. Those are the models using the concept of Photosynthetic Unit (PSU), called also Photosynthetic Factories (PSF) (Prezelin, 1981; Megard et al, 1984; Eilers and Peeters, 1988; Zonneveld, 1997, 1998, Camacho Rubio et al, 2003). The PSF is defined as the sum of light trapping system, reaction centres and associated apparatus, which are activated by a given amount of light energy to produce a certain amount of photoproduct. In spite of the Gargantuan lumping, this definition keeps open the possibility of giving a fair representation of many of the characteristics of

the actual photosynthesis apparatus, and even enables to integrating into the model some measurable intracellular variables, as the concentration of chlorophyll a, cytochrome, D1 protein, etc. (Zonneveld 1997, 1998; Camacho Rubio et al, 2003). The PSF has three states, the open state (indicating that photons can enter the PSF) called  $x_1$ , the activated state (closed) called  $x_2$ , and the inhibited, or non-functional state called  $x_3$ . The PSF in resting or open state can be stimulated and transferred to the activated state when it captures a number of photons required for excitation. The PSFs in activated state have two possible paths, either receiving additional photons and become inhibited, or passing the gained energy to acceptors to start the photosynthesis at a rate controlled by enzymatic systems, and return to the open state. The inhibited PSF can eventually recover, returning to the open state. Those transitions have been schematized in Fig. 2, where  $a_1$ ,  $a_2$  and  $a_3$  indicate the amount of PSU that are in state  $x_1$ ,  $x_2$  and  $x_3$  respectively. In a photo-adapted system the total amount of PSUs ( $a_1 + a_2 + a_3$ ) will remain constant. The kinetics of the different transitions between the states of the PSU may differ in the approaches of different researchers but this does not imply necessarily a conceptual change. The formulation used in each approach by several of those researchers can be seen in Table 1. The rates appearing in the table are those indicated in the scheme of Fig. 2, including biomass synthesis,  $r_b$ , and maintenance,  $r_m$ . Fig. 2 does not take into consideration changes associated with photo-adaptation, which are indicated in Table 1 as  $r_{Chl}$  the rate of change of Chlorophyll per cell. Very few quantitative relationships on light adaptation are available. Perhaps the first one was the following equation, efficiently used by Aiba et al. (1983):

$$\frac{dChl}{dt} = k_1 \cdot (Chl_{\max} - Chl) - k_2 \cdot Chl \quad (2)$$

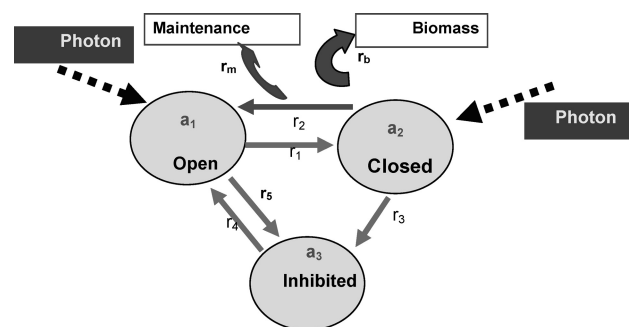


Fig. 2 – Scheme Eilers-Peeters model for photosynthesis. The three possible states of the PSU are shown, together with the rates of the different steps.  $r_1$  is the rate of light energy capture,  $r_2$  the rate of biomass production,  $r_3$  the rate of PSU inhibition,  $r_4$  the rate of inhibited PSU recovery, and  $r_5$  the rate of energy spending in cell maintenance.

Table 1 – Kinetic expressions proposed for the different steps for the application of the PSU models

Step	Eilers-Peeter	Wu-Merchuk	Camacho Rubio et al, 2003	Zonneveld
$r_1$	$\alpha I a_1$	$\alpha I a_1$	$\alpha I a_1 / (K_1 + a_2)$	$\alpha I a_1$
$r_2$	$\beta a_2$	$\beta a_2$	$\beta a_2$	$\beta a_2$
$r_3$	$\gamma I a_2$	$\gamma I a_2$	$\gamma I^{0.5} a_2$	$\gamma I a_2$
$r_4$	$\delta a_3$	$\delta a_3$	$\delta a_3$	$\delta a_3$
$r_5$	–	–	$\beta a_2$	$\beta a_2$
$r_b$	$\beta a_2$	$\beta a_2$	$\beta a_2$	$\beta a_2$
$r_m$	–	–mx	–	–
$r_{Chl}$	–	–	–	–

where *Chl* is chlorophyll-a content in algal cells,  $Chl_{max}$  the maximum value of chlorophyll-a content in algal cells,  $k_1$  and  $k_2$  are rate coefficients of chlorophyll-a synthesis and degradation respectively.

Thus, in spite of huge extent of simplification, the concept of PSU retains the prospect of representing some of the characteristic of the photo-system that most counts in photobioreactor behaviour: the fast response to sudden changes in illumination, the saturation of the reaction centres in PSII, the interconnection of the fast photon-associated reactions, the slower dark reactions leading to biomass synthesis, the photo damage due to high photon flux density (PFD) and the recovery of the damaged D1 proteins.

### Photosynthesis in the bioreactor

The most unique aspect of light as a substrate is that its availability depends not only on the rate of light input, but also on space (distance from the illuminated face). The exponential decay of the irradiance as the distance from the illuminated face increases creates three zones with different regimes of growth in each. A first zone, which extends from the illuminated wall till the point where the light energy arriving just balances the energy needed for growth at the maximum rate ( $I_f$ ). In this zone, the growth rate would be independent of irradiance, which is in excess, and will depend on the cell identity and on the medium composition. This picture is further complicated, however, by photoinhibition, that may lead to a decrease in growth rate near the light source. A second zone that finishes at the point where the light energy arriving just balances

the energy needed for maintenance ( $I_2$ ). In this zone, light is the limiting substrate and the photosynthetic rate will be proportional to  $I$ . The third, poorly illuminated zone where growth will be negative because of lack of enough light.

In each stage a simple exponential decay of irradiance is usually assumed. More sophisticated approaches have been proposed and elaborated as well (Cassano et al, 1995; Cornet et al, 1995, 1998; Pottier et al., 2005)

Several mathematical models of photobioreactors based in this scheme of light decay were proposed. The general problem of photo-reactor design considering light attenuation has been extensively discussed by Bernardez et al. (1987). Several mathematical descriptions of photobioreactors have taken into consideration the distribution of light in the volume of the culture, either using an averaged value of the irradiance, or averaging the growth rate (Dermoun et al., 1992; Evers, 1991; Frohlich et al., 1983; Molina Grima et al., 1993; Molina Grima et al., 1996).

None of the above takes into explicit account the fluid dynamics in the bioreactor. The importance of this element can be supported considering the time constants that appear in the analysis of the photosynthetic process and the dynamics of the reactor, as shown in Fig. 3. This figure is based on Lam et al. (1986) and Lam and Bungay (1986). The figure shows the chain of processes that lead from photon capture to organic molecule synthesis, covering an extremely extended range of time constants. In the figure, the time constants of the steps occurring inside the cell are indicated in parallel to the characteristic times of the fluid dynamics in the bioreactor. It can be seen that the time scale of CO<sub>2</sub> fixation in the process, which corresponds to biochemical dark reactions in the cell, is of the order of

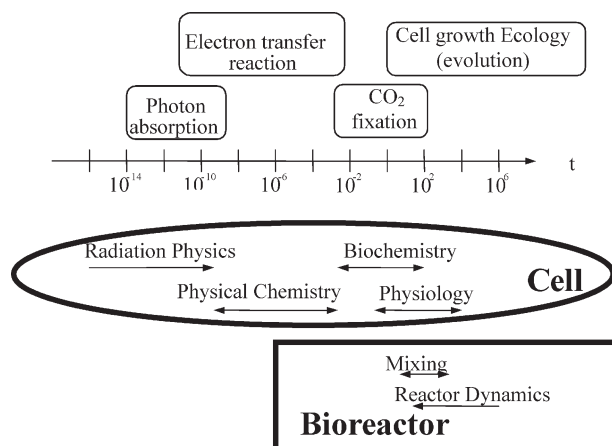


Fig. 3 – Comparison of the time constants of the processes occurring in the cell during photosynthesis and of the fluid dynamics in bioreactors

magnitude of the time constants for bioreactor dynamics. This is required, from the point of view of process dynamics, to make possible the interaction of these two processes. The aim in the present paper is presenting and comparing some examples in integrating kinetics and fluid dynamics in the modeling of photobioreactors.

### Simulated illumination/darkness cycles

In an actual bioreactor, suspended photosynthetic cells move in a more-or-less chaotic way from the high illumination zones to the less illuminated ones. The simplest way of mimicking this type of cell history would be assuming that a certain cycle is repeated time and again by the cell. This cycle is taken as representative for the liquid flow in the photobioreactor as a whole. This approach can easily be modelled mathematically and the calculation is straightforward. Moreover, such a system can be actually built in the laboratory and true measurements can be done of the main variables. Such experimental device has proven to be an extremely useful tool for basic studies on photobioreactor design. Studies of this type, where thin cultures are used in order to avoid self shading by the cells and the light intensity perceived by all the cells in the culture is the same and is measurable, have been first used by Lee and Pirt (1981). Terry (1986) first proposed a methodology for the definition of the illumination cycles. While this has been generally accepted, caution should be used respect the conditions of cycle frequency and illumination where light/dark cycles result in efficiency gain (Janssen et al, 2000, 2001, 2002). Latter on, Wu and Merchuk (2001) combined light/darkness cycles with Eilers and Peeters PSU model (1988). In order to do so, a thin-film photobioreactor where the cells passed repeatedly over an overall 45 s period with varying proportions of light and darkness was built. Fig. 4 shows schematically how the amount of PSU in state 2 would periodically change after the system had entered the pseudo steady state. In the figure it has been assumed that the PSU reaches light saturation during the illuminated period, but this is not necessary the case in general.

These experiments were used to calibrate the mathematical model, and the kinetic constants obtained allowed the calculation of Fig. 5. The figure shows the results produced by the model in terms of the observed specific growth rate,  $\mu$ , as a function of  $t_l/t_c$ , the fraction of cycle time spent in light conditions, for a fixed value of irradiance  $I$ . Each line shows how  $\mu$  would change, for the same cycle length of 45 seconds, as the light time increases from

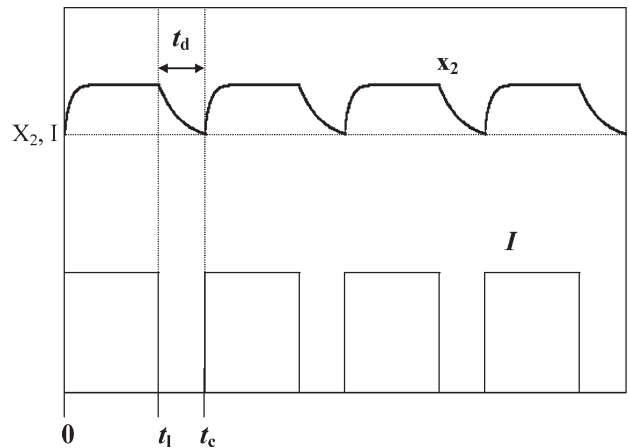


Fig. 4 – Scheme of the variation of the fraction of activated PSU as a response of cyclic changes in illumination

zero to 100 %. The observed growth rate,  $\mu$ , increases monotonically with illumination fraction for lower values of  $I$ . For  $I = 220 \mu\text{Em}^{-2}\text{s}^{-1}$  the curve shows a plateau when the illumination fraction approaches unity, and for higher irradiance a clear maximum appears. The simulation also shows that for higher values of  $I$  the location of the maximum keeps shifting towards lower values of  $t_l/t_c$ . In other words, the higher the irradiance, the longer is the dark period that can be afforded by the system without loss of growth. This is due to the growth inhibition caused by high irradiance, and its reversible character. For greater values of  $I$ , more PSFs reach the closed state, and the dark period allows the repair of damage leading to more PSF in the productive states.

The information presented in Fig. 5 allowed the drawing of what the authors called “island of existence” (Wu and Merchuk, 2001), the area on

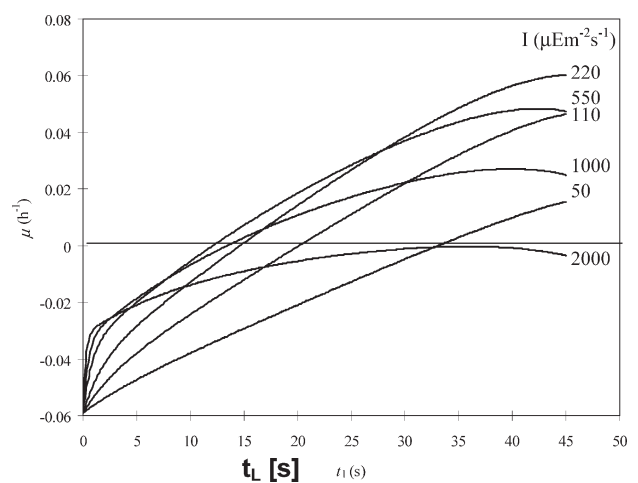


Fig. 5 – Rate of photosynthesis in a thin film bioreactor as a function of the fraction of light during a 45 s cycle, for several values of the illuminance (Wu and Merchuk, 2001)



the plane Illumination fraction/Irradiance where a photobioreactor could operate at steady state.

While those results are of great interest, they correspond to an over-simplified scheme, since not only is the whole illumination story of the cells represented by one single cycle, but the illumination changes are extreme, from maximal  $I$  to complete darkness. In the following section, some of the attempts of a more realistic description will be reviewed.

## The bubble column (BC)

Bubble columns are one of the most popular types of reactors because of reasons related to construction and operation simplicity (Deckwer, 1985). This type of reactors is frequently used to carry out photosynthetic processes. Inside the BC, the light history of the suspended photosynthetic cells is controlled by the fluid dynamics. Therefore, a description of the fluid dynamics in the bubble column is required for an adequate representation of the process. Several flow models for bubble column reactor have been postulated, such as circulation cell model (Joshi and Sharma, 1979), cylindrical eddies model (Zehner, 1986), single internal loop model (Hills, 1974; Ueyama and Miyauchi, 1979), radial distribution model (Clark *et al.*, 1987), and others. More recently, Camacho Rubio *et al.* (2004) provided a method for simultaneously quantifying axial and radial dispersion coefficients. The latter was shown to be important for establishing the frequency of light-dark cycling of the fluid in bubble column photobioreactors and may be useful for the design of other column-type photoreactors.

Hydrodynamic parameters such as gas holdup and the bubble size can affect internal irradiance inside the bubble columns (Sánchez Mirón *et al.*, 1999) and consequently the light history of cells. Under outdoor conditions, presence of gas bubbles generally enhances internal irradiance when the sun is low on the horizon. Near solar noon, the bubbles diminish the internal column irradiance relative to the ungasged state. The effect of aeration on internal irradiance diminishes as the gas flow rate is reduced; however, even at low superficial gas velocities corresponding to a fractional gas holdup below 1%, the irradiance level is affected by up to 15 % relative to gas-free operation. Therefore, for best performance, bubble columns need to be operated at the highest feasible aeration rates consistent with the shear tolerance of the microalga; however, the aeration rate must not be so high as to produce a gas holdup level that prevents light transmission through the column.

Wu and Merchuk (2002) simulated algal growth in a BC of a given radius  $R$ . The main information required for such a simulation is the frac-

tion of the time that a photosynthetic element spends at each light intensity. This was represented by means of a typical trajectory. The trajectory was assumed to follow a circulation cell of the type defined by Joshi and Sharma (Joshi and Sharma, 1979). In order to simplify the calculations, the relationship between the time ( $t$ ) and radial position ( $z$ ) of the cell was assigned to be a cosine function:

$$t = \frac{R}{2} \left( 1 - \cos \frac{2\pi}{T} t \right) \quad (3)$$

The cycle time  $T$  was obtained using the surface renewal model proposed by Danckwerts (1951). The rate of renewal of elements at the wall of the bubble column was evaluated using available data on heat transfer rate through the walls of a bubble column and the Colburn analogy (Colburn, 1933). Limiting this analogy to heat and mass transfer, it can be expressed as (Foust *et al.*, 1979)

$$\frac{1}{\rho C_p} \frac{h}{Pr^{2/3}} = k_L \cdot Sc^{2/3} \quad (4)$$

Equation (4) relates the mass transfer coefficient  $k_L$  to the heat transfer coefficient,  $h$ , and the physical properties of the system. The heat transfer coefficient in bubble columns was evaluated by the following equation, which has proven to be successful over a wide range of reactor dimensions and liquid properties (Zaidi *et al.*, 1990):

$$St = 0.1 \cdot (\text{Re} \cdot \text{Fr} \cdot \text{Pr}^2)^{1/4} \quad (5)$$

and thus the mean surface residence time can be estimated.

The authors assumed the distribution of contact times originally proposed by Danckwerts in his surface renewal model (1951):

$$\Phi(t) = s \cdot e^{-st} \quad (6)$$

This distribution was discretized considering three fractions with three different contact times: one equivalent to all the elements having residence time shorter than  $t_1$ , the second equivalent to all elements having contact times between  $t_1$  and  $t_2$ , and the third one equivalent to all the elements with contact times longer than  $t_2$  (Fig. 6). These fractions will be:

$$\begin{aligned} F1 &= 1 - e^{-st_1} \\ F2 &= e^{-st_1} - e^{-st_2} \\ F3 &= 1 - F1 - F2 = e^{-st_2} \end{aligned} \quad (7)$$

Mean renewal time representative of each of these fractions can be calculated as:

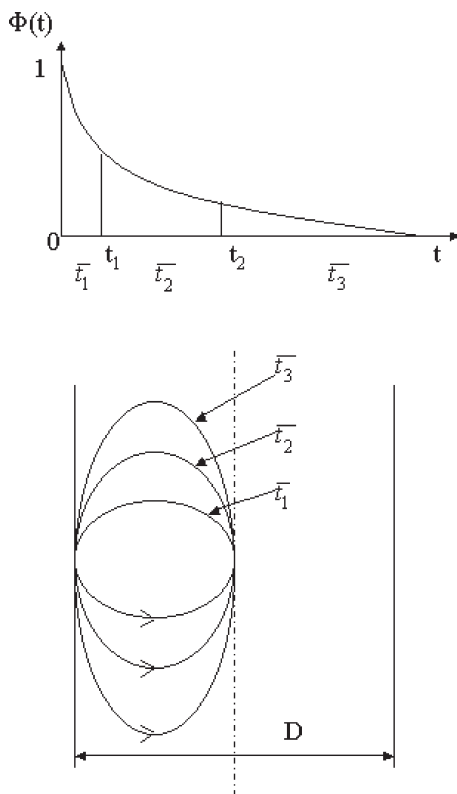


Fig. 6 – The cycles postulated as representing the light/dark cycles in a bubble column (Wu and Merchuk, 2002)

$$\begin{aligned} \bar{t}_1 &= \frac{\frac{1}{s} - \left(t_1 + \frac{1}{s}\right)e^{-st_1}}{F1} \\ \bar{t}_2 &= \frac{\left(t_1 + \frac{1}{s}\right)e^{-st_1} - \left(t_2 + \frac{1}{s}\right)e^{-st_2}}{F2} \\ \bar{t}_3 &= \frac{\left(t_2 + \frac{1}{s}\right)e^{-st_2}}{F3} \end{aligned} \quad (8)$$

The cells travelling along the different trajectories return to the starting point together. The following relationship between the duration of the three trajectories was adopted arbitrarily

$$\bar{t}_3 = 3\bar{t}_2 = 12\bar{t}_1 \quad (9)$$

so that after the longest of the times ( $t_3$  in this case), the second fraction has completed 3 cycles and the first (and fastest) fraction 12 cycles, and all the elements have come together. At this moment the updated biomass concentration was evaluated and a new series of cycles begins.

The light intensity as a function of culture depth was estimated by using Lambert-Beer law:

$$I(t) = I_0 \cdot e^{-(k_x x + k_w)z} \quad (10)$$

This light history of the photosynthetic cells was integrated with the modified (maintenance added) Eilers & Peeters model (1988). The results are presented as a function of “Ground Productivity”. Instead of plotting the biomass concentration of a single reactor, an assembly or “farm” of photobioreactors was considered. The total biomass obtained at the end of a batch culture per unit area of ground required and per unit time (ground productivity,  $P_g$ ) was considered. It was assumed that in addition to the area required for the column itself, which depends on  $D_c^2$ , there is a certain distance required between adjacent column installations,  $L$ , to allow man passage for operation maintenance and to reduce self-shading among adjacent columns. According to these assumptions, the productivity per unit area can be defined as:

$$P_g = \frac{D_c^2 \cdot H}{(D_c + L)^2} \frac{(x_f - x_0)}{\Delta t} = P_D \cdot H \cdot \frac{\Delta x}{\Delta t} \quad (11)$$

The effect of the light intensity and column diameter on the growth is studied and shown in Fig. 7. The simulation is for the superficial gas velocity of 0.0032 m/s. The figure shows the area productivity versus column diameter at different PFD. For each PFD,  $P_g$  firstly increases with the increase of column diameter, reaches a peak, and then goes down. When the effect of irradiance on  $P_g$  for a constant  $D_c$  is examined, the picture depends on the  $D_c$ : For  $D_c < 0.2$  m, the ground productivity increases as the PFD increases till 1000  $\mu\text{Em}^{-2}\text{s}^{-1}$ . The curve of PFD 1500  $\mu\text{Em}^{-2}\text{s}^{-1}$  shows a lower value of  $P_g$ . The curve corresponding to an irradiance of 2000  $\mu\text{Em}^{-2}\text{s}^{-1}$  is much lower at small column diameters, and  $P_g$  begins to increase only when the diameter is around 0.2 m. This fact is important for photobioreactor design when considering the design of a plant. Diameters that could be unpractical at the low irradiance usually utilized in laboratories, may give good productivity in the range of PFD of natural illumination.

A closer examination of Fig. 7 reveals that the maximum of each curve occurs at different column diameter. This indicates that the simulations can be an important tool for the detailed design of of the photobioreactor. Fig. 8 is even more revealing, because it shows the influence of the gas superficial velocity  $J_G$  on  $P_g$  as a function of the PFD for three diameters. It is important to stress that those two variables, gas superficial velocity and tube diameter, appear in the model via the consideration of the flow patterns in conjunction with the kinetic model.

A further refinement of the concept of photobioreactor farm was proposed by Sánchez Mirón et

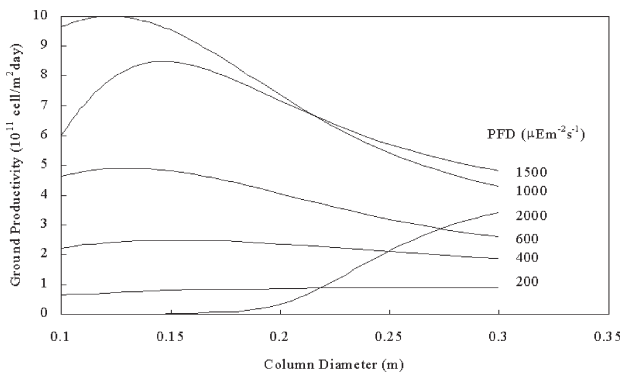


Fig. 7 – The ground productivity of a farm of photobioreactors as a function of the diameter of the bubble column, for several values of the illuminance (Wu and Merchuk, 2002)

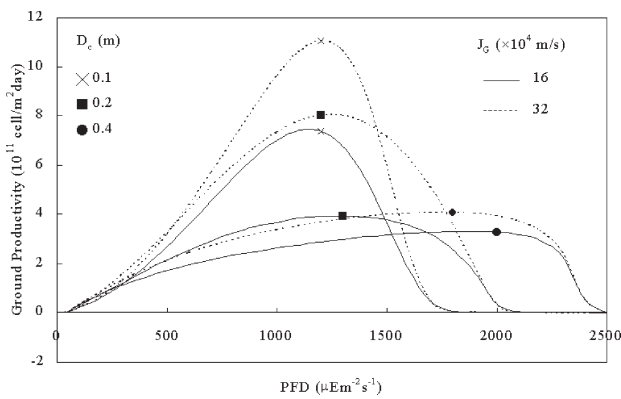


Fig. 8 – The ground productivity of a farm of photobioreactors as a function of the illuminance, for different values of column diameter and gas superficial velocity (Wu and Merchuk, 2002)

al. (1999). The maximum number of the vertical column reactors that may be accommodated in a given area depends on the height of the column which, together with the position of the Sun, establishes the maximum extent of column shadow on the ground. The length of the shadow from the column’s base is given by

$$L_s = \frac{H}{\tan \theta_i} \tag{12}$$

where  $H$  is the height of the column and  $\theta_i$  is the angle of incidence of the direct solar radiation. The angle of incidence—the inclination of the Sun from the normal to the vertical axis of the bubble column—depends on the geographic latitude,  $\phi$ , the day of the year  $N$ , and the solar hour  $h$ ; the angle of incidence is given as (Liu and Jordan, 1960):

$$\theta_i = 90^\circ - \cos^{-1}(\cos \delta \cdot \cos \phi \cdot \cos \omega + \sin \delta \cdot \sin \phi) \tag{13}$$

where  $\phi$  is the geographic latitude. The angles  $\omega$  and  $\delta$  are related to the solar hour and the day of the year (Liu and Jordan, 1960), respectively, as follows:

$$\omega = 15 \cdot (12 - h) \tag{14}$$

and

$$\delta = 23.45 \cdot \sin\left(\frac{360 \cdot (284 + N)}{365}\right) \tag{15}$$

The loci of the maximum extent of the shadow of a 2.6 m tall bubble column are plotted in Fig. 9 for representative days in winter, spring, and summer seasons at a given geographic location. The maximum extent of the shadow in January is about 9 m, whereas the maximum extent in July is about 1.5 m. These distances are measured north-south between parallel east-west lines passing through the base of the vertical column and the tip of the column’s shadow. Ideally, parallel east-west rows of bubble columns should be spaced by at least the maximum length of the shadow in winter. This would assure that the reactors are never mutually shaded, however, a more optimal setup would place the rows of reactors closer, about midway between the high extremes of the shadow length in the summer and the winter. Consequently, there will be no mutual shading in the summer but some shading would occur during the winter. In a single east-west row of columns the columns could be spaced quite close together. Close spacing within east-west rows has no impact on illumination, but it improves efficiency of land use. The optimal column height will also depend not only on technical considerations such as wind speed and strength of optically transparent materials used, but also on the impact of height on fluid dynamics.

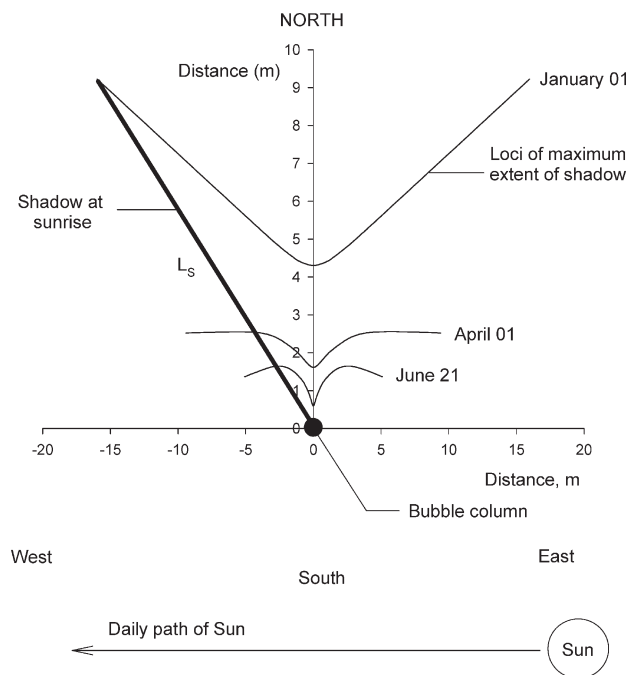


Fig. 9 – The loci of the maximum extent of the shadow of a 2.6 m tall bubble column in a farm of photo-bioreactors (Sanchez-Mirón et al., 1999)

### The Air Lift Reactor (ALR)

ALRs are completely different from BCs in their fluid dynamics. Instead of the quasi chaotic movement in the BC, the ALR offers an overall ordered flow through defined ducts that are built with this purpose in mind. If the configuration of concentric tubes is chosen and the light source is at the external wall, the internal draft tube delimits an area that is inherently the darkest. Wu and Merchuk (2004) simulated algal growth in the ALR combining an analytical solution of the equations and finite elements calculation, assuming that the downcomer was divided into several radial regions according to the prevailing PFD. Each interval has a constant PFD and the change in irradiance from region to region is  $\Delta I$ . Fig. 10 illustrates the light intervals. Fig. 11 shows how the model was able to fit successfully the results obtained in a bench-scale ALR, including the effect of gas superficial velocity  $J_G$ .

In Fig. 12, the combined effects between the two main design variables of an ALR,  $A_r/A_d$  (area ratio) and  $H_d$  (column height) are presented. Those variables influence the flow patterns in the reactor

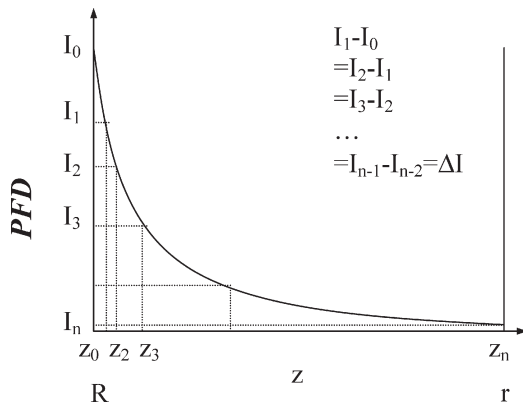


Fig. 10 – The mean discrete distribution adopted for the light in the annulus of the ALR (Wu and Merchuk, 2004)

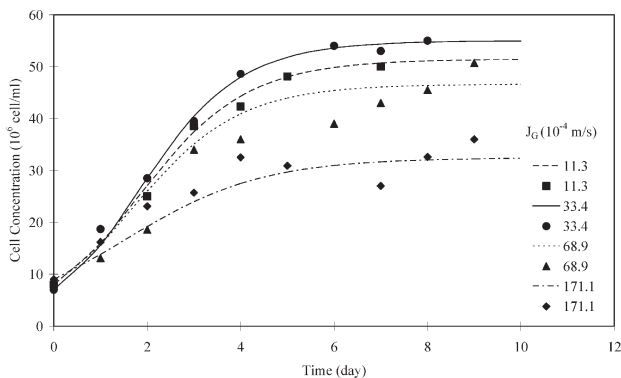


Fig. 11 – Predicted vs. measured final cell concentrations in an ALR, for four different gas superficial velocities (Wu and Merchuk, 2004)

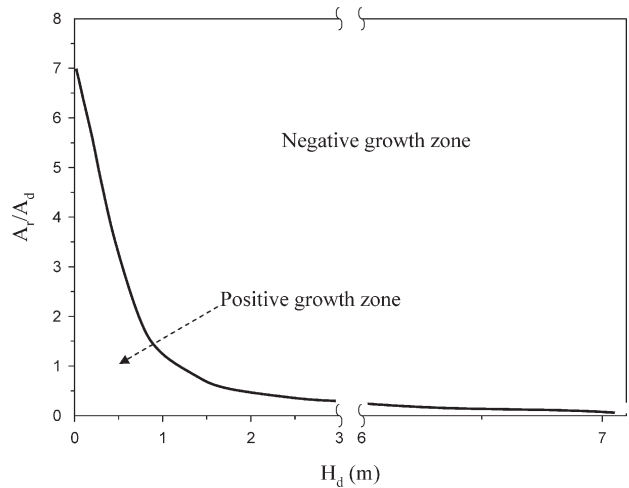


Fig. 12 – The zones of positive photosynthetic growth in an ALR, on the plane defined by the cross sectional areas  $A_r/A_d$  and the column height  $H_d$  (Wu and Merchuk, 2004)

and determine in fact the illumination history of the cells. The solution obtained by Wu and Merchuk (2004) show that there is an area on the  $A_r/A_d-H_d$  plane where net growth is not possible, and in consequence both variables should be manipulated by the designer to place the photobioreactor inside the zone of sustained growth. This is another version of the previously mentioned “island of existence”. The plane where the map is drawn in this case is however related only to design variables that determine the illumination cycles, and will correspond to given conditions of light and gas flow rate.

### Tubular photobioreactors

Tubular photobioreactors consist of straight, coiled or looped transparent tubing arranged in various ways for maximizing sunlight capture. Phototrophic cultures are circulated through the tubes by various methods; use of airlift circulators is especially common. Molina Grima et al. (1999, 2000) developed a method for relating the light/dark frequency to prevailing hydrodynamics and irradiance level in a tubular photobioreactor. The light zone is also defined as that in which the light intensity is at saturation value, or greater, and the dark zone is one where the light intensity is below the saturation threshold. Dependence of culture biomass productivity ( $P_b$ ) on light/dark cycle frequency ( $\nu$ ) was found to be a Monod type growth equation given by:

$$P_b = \frac{P_{b\max} \cdot \nu}{K_\nu + \nu} \tag{16}$$

where  $P_{b\max}$  is the maximum biomass productivity,  $\nu$  the light/dark cycle frequency, and  $K_\nu$  the frequency for half the maximum productivity. Both



$P_{b\max}$  and  $K_v$  showed a linear dependence on the day-averaged irradiance measured on the reactor's surface ( $I_0$ ) given by:

$$P_{b\max} = a + b \cdot I_0 \quad (17)$$

$$K_v = c + d \cdot I_0 \quad (18)$$

where  $a$  to  $d$  are constants.

The frequency was calculated as

$$\nu = \frac{1 - \phi_f}{t_d} \quad (19)$$

being  $t_d$  the time spent in the dark zone and  $\phi_f$  is the fractional culture volume that is illuminated (i.e. the photic volume fraction) for a known level of external irradiance, biomass concentration, and absorption coefficient of the biomass, that can be estimated from the light profiles;  $\phi_f = V_f / (V_f + V_d)$ . The values of  $t_d$  were calculated as

$$t_d = \frac{d_t \cdot (\theta - \sin \theta)}{2 \cdot U_R \cdot \sin \theta} \quad (20)$$

where  $d_t$  is the tube diameter,  $U_R$  is the radial velocity and  $\theta$  is a specific angle necessary for calculating  $\phi_f$ . Since, cells move radially with the fluid because of momentum transport between the turbulent core and the more quiescent boundary layer adjacent to walls, a radial velocity was approximated as the characteristic velocity of turbulence in the center of the tube:

$$U_R = 0.2 \cdot \left( \frac{U_L^7 \cdot \mu}{d_t \cdot \rho} \right)^{1/8} \quad (21)$$

which allows the calculation of  $U_R$  in the turbulent core as a function of the superficial liquid velocity ( $U_L$ ), the tube diameter ( $d_t$ ), and the density ( $\rho$ ) and viscosity ( $\mu$ ) of the culture broth.

Biomass productivity data are shown in Fig. 13 as a function of light/dark cycle frequency day-averaged irradiance is shown. Experimental data were obtained from two outdoor placed tubular photobioreactors with tube internal diameters of 0.053 m and 0.025 m and operated as continuous cultures at various dilution rates. Scale-up capability was also proved using the criterion of keeping constant the light/dark cycle frequency in reactors of different diameters.

Other attempts have been done following the approach presented here (Luo and Al-Dahann, 2004; Pruvost et al, 2002, Muller-Feuga et al, 2002, 2003, Potier et al, 2005). The present paper is not meant to be an exhaustive report, but to enlighten the main principles of the approach of integrating kinetic models of photosynthesis and flow patterns

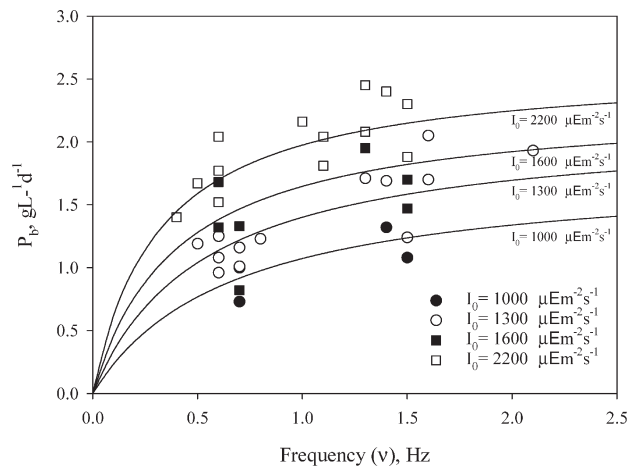


Fig. 13 – Biomass productivity data in a tubular photobioreactor as a function of light/dark cycle frequency day-averaged irradiance (Molina Grima et al, 2000)

that define the light history of the cells in photobioreactors.

### Summary

While many of the photobioreactors in operation today are based more on invention than on engineering design, the knowledge basis available on the modelling of photosynthetic systems has advanced sensibly in the last time. The public interest on sustainability provides a positive vector pressing toward the application of this knowledge. One of the most important elements that has to be integrated into the design is the fluid dynamics and the influence of the flow patterns on the yield of the photosynthetic systems. Several examples of the ways in which the integration of fluid dynamics and photosynthesis kinetics can be carried out are presented in the present review.

### ACKNOWLEDGEMENT

Authors acknowledge the support of the Ministerio de Educación y Ciencia de España (Programa de ayudas para estancias de profesores e investigadores en España SAB-2005-0064 and Project AGL2005-07924-C04-04), and of the Department of Chemical Engineering, Universidad de Almería.

### Nomenclature

- $Chl$  – chlorophyll-a content in algal cells ( $g\ m^{-3}$ )
- $Chl_{\max}$  – maximum value of chlorophyll-a content in algal cells ( $g\ m^{-3}$ )
- $C_p$  – Heat capacity ( $cal \cdot g^{-1}\ K^{-1}$ )
- $d_b, D_c$  – tube diameter, (m)

F1, F2, F3 – discrete time distributions, Eq. 7

H – column height, (m)

I – Irradiance ( $E\ m^{-2}\ s^{-1}$ )

$k_1$  – rate coefficient of chlorophyll-a synthesis, ( $s^{-1}$ )

$k_2$  – rate coefficient of chlorophyll-a degradation, ( $s^{-1}$ )

kx, kw – Light attenuation constants related to biomass and water, respectively, Eq. 10

$k_L$  – mass transfer coefficient, ( $m\ s^{-1}$ )

$K_i$  – frequency for half the maximum productivity, ( $s^{-1}$ )

$L_s$  – length of shadow, (m)

m – maintenance, ( $s^{-1}$ )

N – day of the year

$P_b$  – biomass productivity, ( $gm^{-3}\ day^{-1}$ )

$P_{bmax}$  – maximum biomass productivity, ( $gm^{-3}\ day^{-1}$ )

$P_g$  – Ground productivity, ( $g\ m^{-2}\ day^{-1}$ )

Pr – Prandtl number (–)

r – reaction rate (Fig 2 and Table 1)

R – Radius of the column, (m)

Re – Reynolds number (–)

Sc – Schmidt number (–)

St – Stanton number (–)

t – time (s)

$\bar{t}_1, \bar{t}_2, \bar{t}_3$  – Mean renewal times for regions 1, 2, 3, Eq. 8, (s)

$t_d$  – time spent in the dark zone, (s)

$t_L$  – time spent in the illuminated zone, (s)

T – cycle time (s)

$U_L$  – liquid velocity into the tube, ( $m\ s^{-1}$ )

$U_R$  – radial velocity, ( $m\ s^{-1}$ )

$x_0$  – initial biomass concentration ( $g\ m^{-3}$ )

$x_f$  – final biomass concentration ( $g\ m^{-3}$ )

### Greek symbols

$\alpha, \beta, \gamma, \delta$  – kinetic constants (Table 1)

$\Delta$  – interval

$\phi_f$  – fractional culture volume that is illuminated (i.e. the photic volume fraction).

$\phi$  – geographic latitude

$h$  – solar hour

$\mu$  – viscosity of the culture broth ( $g\ m^{-1}\ s^{-1}$ ), specific growth rate ( $s^{-1}$ )

$\mu_{max}$  – Maximal specific growth rate ( $s^{-1}$ )

$\delta$  – declination the angular position of the Sun at solar noon with respect to the plane of the equator, north positive.

$\Phi$  – Surface renewal distribution function, ( $s^{-1}$ )

$\theta$  – specific angle necessary for calculating

$\theta_i$  – angle of incidence of the direct solar radiation

$\nu$  – Light/dark cycle frequency, ( $s^{-1}$ )

$\rho$  – density of the culture broth, ( $g\ m^{-3}$ )

$\omega$  – angle corresponding to the solar hour

### References

1. Aiba, S., (1982) Growth kinetics of photosynthetic microorganisms. *Adv. Biochem. Eng.* **23**: 85-156.
2. Aiba, S., Okada, M., Sudo, R., Ogawa, T., Sekine, T., (1983) Siltulation of water-bloom in a eutrophic lake-I. Photosynthetic characteristics of *microcystis aeruginosa*. *Water Res.* **17**(8): 869-876.
3. Bernardez, E. R., Claria, M. A., Cassano A. E., (1987) Analysis and design of photoreactors. In: Carberry JJ, Varma A. (eds.), *Chemical Reaction and Reactor Design*. Marcel Dekker, N. Y.
4. Camacho Rubio, F., García Camacho, F., Fernandez Sevilla, J. M., Chisti, Y., Molina Grima, E., (2003) A mechanistic model of photosynthesis in microalgae, *Biotechnol. Bioeng.* **81**(4): 459-473.
5. Camacho Rubio, F., Sánchez Mirón, A., Cerón García, M. C., García Camacho, F., Molina Grima, E., Chisti, Y., (2004) Mixing in bubble columns: a new approach for characterizing dispersion coefficients. *Chem. Eng. Sci.* **59**: 4369-4376.
6. Cassano, A. E., Martin, C. A., Brandi, R. J., Alfano, O. M., (1995) Photoreactor analysis and design: fundamentals and applications. *Ind. Eng. Chem. Res.* **34**(7): 2155-2201.
7. Clark, N. N., Atkinson, C. M. F., Lemmer, R. L. C., (1987) Turbulent Circulation in Bubble Columns. *AICHE J.* **33**: 515-518.
8. Colburn, A. P., (1933) A Method of Correlating Forced Convection Heat Transfer Data and a Comparison with Fluid Friction. *Trans. Am. Inst. Chem. Eng.* **29**: 174-209.
9. Cornet, J. F., Dussap, C. G., Gros, J. B., (1995) A simplified monodimensional approach for modeling coupling between radiant light transfer and growth kinetics in photobioreactors. *Chem. Eng. Sci.* **50**(9): 1489-1500.
10. Cornet, J. F., Dussap, C. G., Gros, J. B., (1998) Kinetics and bioenergetics of microorganisms in photobioreactors: application to Spirulina growth. *Adv. Biochem. Eng. Biotechnol.* **59**: 155-224.
11. Danckwerts, P. V., (1951) Significance of liquid-film coefficients in gas absorption, *Ind. Eng. Chem.* **43**: 1460-1467.
12. Deckwer, W. D., (1992) *Bubble Column Reactors*. Chichester, John Wiley.
13. Dermoun, D., Chaumont, D., Thebault, J., Dauta, A., (1992) Modeling of growth of *Porphyridium cruentum* in connection with two interdependent factors: light and temperature. *Bioresource Technol.* **42**: 113-117.
14. Eilers, P. H. C., Peeters, J. C. H., (1988) A model for the relationship between light intensity and the rate of photosynthesis in phytoplankton. *Ecol. Modeling.* **42**: 199-215.
15. Evers, E. G., (1991) A model for light limited continuous cultures. *Biotechnol. Bioeng.* **38**: 254-259.
16. Foust, A. S., Wenzel, L. A., Clump, C. W., Maus, L., Andersen, L. B., (1979) *Principles of unit operations*. 2nd edition. John Wiley & Sons, New York.
17. Frohlich, B. T., Webster, I. A., Ataai, M. M., Shuler, M. L., (1983) Photobioreactors: Models for interaction of light intensity, reactor design and algal physiology. *Biotech. Bioeng. Symp.* **13**: 331-350.
18. Geider, R. J., MacIntyre, H. L., Kana, T. M., (1998) A dynamic regulatory model of Phytoplankton acclimation to light, nutrients and temperature. *Limnol. Oceanogr.* **43**(4): 679-994.
19. Harmon, R., Challenor, P., (1997) A Markov chain Monte Carlo method for estimation and assimilation into models. *Ecol. Modell.* **101**(1): 41-59.
20. Hills, J. H., (1974) Radial Non-uniformity of Velocity and Voidage in a Bubble Column. *Trans. Inst. Chem. Eng.* **52**: 1-9.

21. Janssen, M., Janssen, M., de Vinter, M., Tramper, J., Mur, L. R., Snel, J., Wijffels, R. H., (2000) Photosynthetic efficiency of *Dunaliella tertiolecta* under short light/dark cycles, *J. of Biotechnology* **78**: 123-137.
22. Janssen, M., Slenders, P., Tramper, J., Mur, L. R., Wijffels, R. H., (2001) Efficiency in light utilization of *Chlamydomonas reinhardtii* under medium-duration light/dark cycles, *Enzyme and Microbial Technology* **29**: 289-305.
23. Janssen, M., Tramper, J., Mur, L. R., Wijffels, R. H., (2002) Enclosed Outdoor Photobioreactors: Light regime, Photosynthetic Efficiency, Scale-Up and Future Prospects, *Biotechnol. Bioengng.* **81**: 193-210.
24. Joshi, J. B., Sharma, M. M., (1979) A Circulation Cell Model for Bubble Columns. *Trans. Inst. Chem. Eng.* **57**: 244-251.
25. Lam, H. L. Y., Bungay, H. R., (1986) Frequency response analysis of oxygen evolution by algae. *J. Biotech.* **4**: 125-142.
26. Lam, H. L. Y., Bungay, H. R., Culotta, L. G., (1986) An engineer look at photosynthesis. *Appl. Biochem. Biotech.* **13**: 37-73.
27. Lee, Y., Pirt, S. J., (1981) Energetics and photosynthetic algal growth. Influence of intermittent illumination in short (40s) cycles. *J. Gen. Microbiol.* **124**: 43-52.
28. Liu, B. Y. H., Jordan, R. C., (1960) The interrelationship and characteristic distribution of direct, diffuse and total solar radiation. *Solar Energy.* **7**: 53–65.
29. Luo, H. P., (2004) Analyzing and modelling photobioreactors by combining first principles of physiology and hydrodynamics, *Biotechnol. Bioeng.* **85**(4): 283-293.
30. Marshall, H. L., Geider, J. G. Flynn, J., (2000) A Mechanistic model for photoinhibition. *New Phytol.* **145**: 347-359.
31. Megard, R. O., Tonkyn, D. W., Senft, W. H., (1984) Kinetics of oxygenic photosynthesis in planktonic algae. *J. Plankton Res.* **6**: 325-337.
32. Molina Grima, E., Ación Fernández, F. G., García Camacho, F., Chisti Y., (1999) Photobioreactors: light regime, mass transfer, and scaleup. *J. Biotechnol.* **70**: 231–248.
33. Molina Grima, E., Fernández Sevilla, J. M., Sánchez Pérez, J. A., García Camacho, F., (1996) A study on simultaneous photolimitation and photoinhibition in dense microalgal cultures taking into account incident and averaged irradiances. *J. Biotech.* **45**: 59-69.
34. Molina Grima, E., Sánchez Pérez, J. A., García Camacho, F., Lopez, A. D., (1993) N-3 PUFA Productivity in Chemostat Culture of Microalgae. *Appl. Microbiol. Biotechnol.* **38**: 599-605.
35. Molina Grima, E., Ación Fernández, F. G., García Camacho, F., Camacho Rubio, F. Chisti, Y., (2000) Scale-up of tubular photobioreactors. *J. Appl. Phycol.* **12**: 355-368.
36. Muller-Feuga, A., Le Guedes, R. Pruvost, J., (2003) Benefits and limitation of modelling for optimization of *Porphyridium cruentum* cultures in an annular photobioreactor. *J. Biotechnol.* **103**(2): 153-163.
37. Muller-Feuga, A., Pruvost, J., Le Guedes, R., Le Dean, L., Legentilhomme, P. Legrand, J. (2003) Swirling flow implementation in photobioreactor for batch and continuous cultures of *Porphyridium cruentum* cultures in an annular photobioreactor. *Biotechnol. Bioeng.* **84**(5): 544-551.
38. Pahlow, M., (2005) Linking Chlorophyll nutrient dynamics to the Redfield N:C ratio with a model of optimal plankton growth. *Marine Ecol. Prog. Series.* **287**: 33-43.
39. Pottier, L., Pruvost, J., Deremetz, J., Cornet, J. F., Legrand, J., Dussap, C. G., (2005) A fully predictive model for one-dimensional light attenuation by *Chlamydomonas reinhardtii* in a torus reactor. *Biotechnol. Bioeng.* **91**(5): 569-582.
40. Prézelin, B. B., (1981) Light reactions in photosynthesis. *Can. J. Fish. Aquat. Sci.* **210**, 1-43.
41. Pruvost, J., Legrand, J., Legentilhomme, P., Muller-Feuga, A., (2002) Simulation of microalgae growth in limiting light conditions-flow effect. *AIChE J.* **48**: 1109-1120.
42. Sánchez Mirón, A. S., Gómez Contreras, A., García Camacho, F. G., Molina Grima, E., Chisti, Y., (1999) Comparative evaluation of compact photobioreactors for large-scale monoculture of microalgae. *J. Biotechnol.* **70**: 249–270.
43. Smith, S. L., Casareto, B. E., Niraula, P. M., Suzuki, P. M., Hargreaves, J. C., Annan, J. D., Yamanaka, Y., (2007) Examining the regeneration of Nitrogen by assimilation data from incubations into multi-elements ecosystem model. *J. Marine Sys.* **64**(1-4): 135-152.
44. Terry, K. L., (1986). Photosynthesis in modulated light: Quantitative dependence of photosynthesis enhancement on flashing rate. *Biotechnol. Bioeng.* **28**: 988-995.
45. Ueyama, K., Miyauchi, T., (1979) Properties of Recirculating Turbulent Two Phase Flow in Gas Bubble Columns. *AIChE J.* **25**: 258-266.
46. Wu, X., Merchuk, J. C., (2002) Simulation of algae growth in a bench scale bubble column reactor. *Biotechnol. Bioeng.* **80**: 156-168.
47. Wu, X., Merchuk, J. C., (2001) A model integrating fluid dynamics in the photosynthesis and photoinhibition process. *Chem. Eng. Sci.* **56**: 3527-3538.
48. Wu, X., Merchuk, J. C., (2004) Simulation of Algae Growth in a Bench Scale internal Loop Airlift Reactor. *Chem Eng. Sci.* **59**: 2899-2912.
49. Zaidi, A., Deckwer, W. D., Mrani, A., Benchechou, B., (1990) Hydrodynamics and heat transfer in three-phase fluidized beds with highly viscous pseudoplastic solutions. *Chem. Eng. Sci.* **45**(8): 2235-2238.
50. Zehner, P., (1986) Momentum, Heat and Mass Transfer in Bubble Columns. Part 1. Flow Model of the Bubble Column and Liquid Velocities. *Int. Chem. Eng.* **26**: 22-29.
51. Zonneveld, C., (1997) Modelling effects of photoadaptation on the photosynthesis-irradiance curve. *J. Theor. Biol.* **186**: 381-388.
52. Zonneveld, C., (1998) Photoinhibition as affected by photoacclimation in phytoplankton: a model approach. *J. Theor. Biol.* **193**: 115-123.

